(Online) ISSN 2712-0562
Sustainable Engineering and Innovation *Original Research*
Vol. 7, No. 2, 2025, pp.403-414
https://doi.org/10.37868/sei.v7i2.id594

Modeling and simulation of electromagnetic interference from 2G–6G mobile phones on implanted cardiac pacemakers

Jaafar Qassim Kadhim[1], Hassan Hamed Naji[2], Sazan K. AL-jaff[3]
[1] Electrical Engineering Department, College of Engineering, Mustansiriyah University, Baghdad, Iraq
[2] Electronic and Communications Departments, Engineering College, University of AL-Qadisiyah, Ad Diwaniyah, Iraq
[3] University of Technology, Baghdad, Iraq

*Corresponding author E-mail: jaafar80@uomustansiriyah.edu.iq

Received Nov. 3, 2024
Revised Jun. 22, 2025
Accepted Aug. 02, 2025
Online Sep. 18, 2025

Abstract
Using cell phones in proximity to implanted sensitive medical electronic devices has raised concerns about the potential negative impacts of electromagnetic interference (EMI) on pacemaker functioning. This study presents a comprehensive simulation-based analysis of induced fields and voltages in pacemaker leads resulting from electromagnetic emissions of 2G through 6G mobile phones. The EMI model incorporates parameters including distance, orientation, frequency, antenna gain, and burst factor. Simulation results show that 2G and 3G phones, particularly within 10-15 cm at 0° alignment, can induce electric fields exceeding the pacemaker immunity threshold of 3 V/m. Conversely, 5G and 6G technologies, due to higher frequencies and directional emissions, exhibit minimal EMI risks. These findings support updated safety guidelines and call for revised EMI testing protocols considering emerging wireless standards.

Keywords: Electromagnetic interference (EMI), Electromagnetic radiated emissions, Implanted pacemakers, Specific absorption rate (SAR)

1. Introduction

Electromagnetic interference (EMI) is defined as the disturbance in an electrical circuit functioning due to the effect of either electromagnetic induction or radiation emitted from external sources in the surrounding environment [1]. In the field of biomedical devices, implantable cardiac pacemakers are designed to monitor and control heart rhythms. These devices are highly sensitive and can be disrupted by unintended electromagnetic exposure [2].

The widespread use of mobile phones in close proximity to the human body makes them one of the most prevalent sources of EMI for implantable devices, leading to potential health risks. As wireless technologies have rapidly progressed from first-generation (1G) to sixth-generation (6G), the electromagnetic environment surrounding the human body has evolved significantly. Each generation introduces variations in frequency bands, modulation techniques, and emission patterns that affect the level and nature of EMI [3, 4]. The choice of the placement of components within electronic systems in the appropriate design plays an important and vital role in reducing EMI, as indicated in previous studies on optimal PCB layout for communication devices [5].

Earlier studies revealed conflicting results regarding EMI impacts, some highlighting significant effects from GSM (2G) signals, while others indicated minimal influence from modern systems. A recent clinical study by

Wisaratapong et al. showed no direct EMI in 5G environments under standard usage conditions but suggested that ringing phones may still cause interference [3]. The study conducted by [6] highlighted that cell phones operating on GSM frequencies have more potential to cause higher levels of EMI compared to those operating on newer technologies. The study carried out by Yaqiong Li et al shows that exposure to 5G base station radiation may affect medical care devices due to short-time strong electromagnetic narrow waves in specific areas [7]. However, most existing works lack rigorous modeling of critical variables such as distance, angle of alignment, burst modulation characteristics, and specific absorption rate (SAR). Furthermore, high-frequency emissions, like those from 5G and 6G systems, exhibit different propagation behaviors such as directional beamforming and rapid radio signal attenuation, which can reduce near-field exposure risk [8-11]. Advanced control and optimization methods, such as neural network-based controllers, have been applied to enhance the stability and performance of power electronics in various applications, demonstrating the potential of intelligent algorithms to improve system robustness against disturbances [12].

This paper develops a mathematical and simulation-based analytical model to assess the EMI effects of 2G through 6G mobile phones on implanted pacemakers. The model quantifies induced voltages and electric field intensities as functions of phone-pacemaker separation, orientation, frequency, antenna gain, and burst characteristics. SAR-based risk analysis is also conducted to map near-field exposure zones. The proposed model enables generation-specific EMI risk characterization and supports the development of updated EMI testing protocols.

The paper is organized as follows: Section 2 reviews the interaction mechanisms of EMI. Section 3 formulates the mathematical model. Section 4 presents the simulation approach, while Section 5 presents the results.

2. Mechanisms of EMI effects on electronic devices

The proliferation of cell phones has raised concerns about electromagnetic interference (EMI) that may affect the performance of nearby medical electronic sensitive devices [13]. Cell phones operate across a wide range of frequencies depending on the generation of wireless technology and geographic region; therefore, cell phones emit radiofrequency (RF) radiation at different frequencies, generating time-varying electromagnetic fields that can couple into nearby medical device circuits via the generated induction interference [14-16].

The magnitude of the induced electric field intensity at a distance d from the cell phone transmitting antenna in the far-field region can be expressed by:

$$E(d) = \frac{\sqrt{30\, P_t\ G_t}}{d} \tag{1}$$

Where $E(d)$ is the electric field strength at a distance d from a cell phone transmit antenna (V/m), P_t is the power transmitted by the cell phone (W), G_t is the cell phone antenna gain (unitless), and d is the distance from the source (m).

The actual induced electric field intensity varies with the orientation angle (θ) or the angle at which the cell phone emission is incident [11].

$$E(d) = \frac{\sqrt{30\, P_t\ G(\theta)}}{d}\ \cos(\vartheta) \tag{2}$$

The cell phone radiates electromagnetic emissions, induces current in sensitive devices, and interferes with their normal operation. The inverse relationship of the induced electric field with distance denotes how proximity to a cell phone significantly affects the exposure level of surrounding electronic devices. EMI effects can be generated even with low power emissions, where the cell phone is sufficiently close to unprotected electronic devices. The level of the induced electric field may exceed the electromagnetic immunity thresholds of certain unprotected or unshelled medical devices [15].

The strength of electromagnetic emissions from mobile phones depends on the power transmitted by the cell phone, which is dynamically controlled based on its distance from the serving base station and environmental obstructions. Cell phones typically emit between 0.25 to 2 watts of RF power. This power may increase in areas with poor reception to maintain signal quality, raising the potential for electromagnetic interference. The transmission of cell phones is typically non-continuous and pulsed. For example, GSM phones transmit in short bursts at a rate of 217 Hz, which can produce periodic EMI [17].

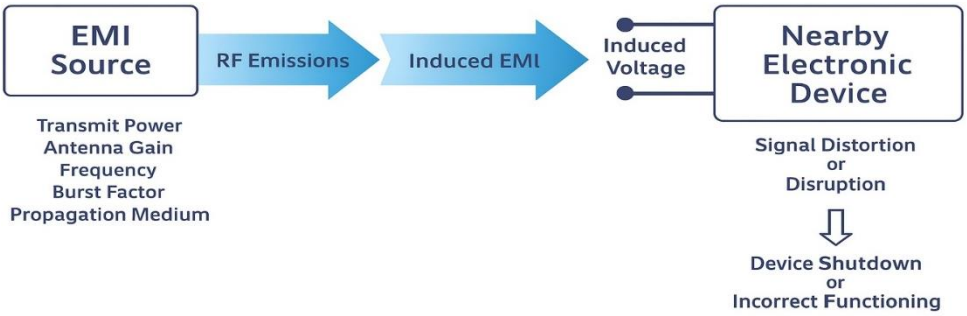

Figure 1. EMI interaction mechanism

The interaction between mobile phone radiation and implanted pacemaker devices occurs through electromagnetic coupling. The radiofrequency (RF) signal emitted by a cell phone can induce alternating currents in a pacemaker's leads, as illustrated in Figure 1. The current or voltage induced in the implanted pacemaker may affect the pacemaker's sensing circuitry, leading to inhibition of pacing [18, 19].

3. Mathematical modeling of EMI effect

Investigate and quantify the effect of external EMI from cell phones interacting with the pacemaker device, electric field attenuation, and the voltage induced at the pacemaker's leads must be evaluated to decide whether this voltage exceeds EMI susceptibility thresholds.

This section presents a mathematical model to understand the coupling mechanisms and to estimate the electromagnetic interference (EMI) effects on implanted cardiac pacemakers across several generations of cellular technologies. The main elements of the model include:

- A cell phone that represents the RF source of EMI emitting modulated electromagnetic waves at specific frequencies and power levels matching the network generations.
- Pacemaker device: represents the victim device, which is designed to deliver pacing pulses. It has conductive wires that act as antennas on which the currents or voltage are induced from an external EMI source (cell phone).

The cell phone is assumed to be located at a distance d from the pacemaker device with an alignment angle (θ) as illustrated in Figure 2. The alignment angle is the angle between the RF field vector and the pacemaker lead longitudinal axis in the signal propagation medium.

The power density (P_d) induced at a distance d due to the emissions from the cell phone antenna is expressed as [20]:

$$P_d = \frac{P_t G(\theta)}{4\pi d^2} \quad (2)$$

Where P_t is the power transmitted through the cell phone antenna that has a gain of (G).

Cell phone antennas are typically not isotropic as they radiate more power in certain directions; therefore, they are characterized by an antenna gain function G (θ). For many directional antennas, the gain is expressed as a function of $\cos^n(\theta)$ [21, 22]. Therefore, the power density (W/m²) at a distance d from the cell phone antenna is:

$$G(\theta) = G_{\max} \cos^n(\theta)$$

$$P_d = \frac{P_t \cos^n(\theta)}{4\pi d^2} \quad (3)$$

Where θ is the angle between the cell phone antenna axis and the implanted pacemaker, which represents the phone's angular direction (radian), and n is an empirical constant that models the transmit antenna directivity or beamwidth.

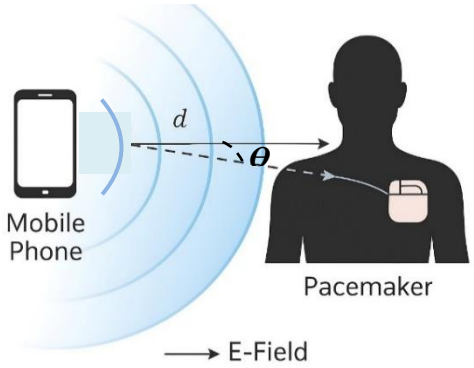

Figure 2. EMI coupling model from cell phone to pacemaker

The power density induced due to RF signal transmission in free space medium is related to the induced electric field (E) through the free space intrinsic impedance (η) by the equation [20]:

$$|E(d)|^2 = P_d \, \eta$$

$$|E(d)|^2 = \frac{P_t \, \eta \cos^n(\theta)}{4\pi d^2} \quad (4)$$

Where $E(d)$ is the electric field intensity at the linear distance (d) from the source, and (η) is the free space intrinsic impedance (120π) Ω.

The electromagnetic interference (EMI) intensity generated by the induced electric field in circuits at a distance d is proportional to the square of the electric field intensity:

$$EMI \propto |E(d)|^2 \propto \frac{P_t \, \eta \cos^n(\theta)}{4\pi d^2}$$

$$E(d) = E(d_o)\left(\frac{d_o}{d}\right) \quad (5)$$

$$|E(d)|^2 = E^2(d_o)\left(\frac{d_o}{d}\right)^2$$

Where d_o is a reference distance that is very close to the source at which the angle (θ) is equal to zero.

$$|E(d_o)|^2 = P_d(d_o)\,\eta = \frac{P_t \, \eta \cos^n(0)}{4\pi (d_o)^2}$$

$$|E(d)|^2 = \frac{P_t \, \eta \cos^n(0)}{4\pi (d_o)^2}\left(\frac{d_o}{d}\right)^2$$

$$|E(d)|^2 = \frac{P_t \eta}{4\pi (d_o)^2} (\frac{d_o}{d})^2 \quad (6)$$

$$EMI \propto |E(d)|^2 \propto \frac{P_t \eta \cos^n(\theta)}{4\pi (d_o)^2} (\frac{d_o}{d})^2$$

$$EMI = \frac{P_t \eta \cos^n(\theta)}{4\pi (d_o)^2} (\frac{d_o}{d})^2 B(f) \quad (7)$$

Where *B (f)* is the burst enhancement factor for a certain generation. This factor can model how time-domain burstiness of the signal enhances EMI risk.

Mobile cell phone manufacturers usually confirm the value of the specific absorption rate (SAR) for their products to verify that the device meets safety standards for radiofrequency (RF) energy exposure. SAR is a measure of the RF energy absorbed by the human biological tissue when using a certain cell phone. SAR is expressed in terms of tissue conductivity (σ), tissue mass density (ρ), and the induced electric field intensity as [23, 24]:

$$SAR = \frac{\sigma E^2}{\rho} \quad (8)$$

$$E(d) = \sqrt{\frac{\rho\, SAR}{\sigma}} (\frac{d_o}{d}) \quad (9)$$

Equation 9 is useful to be applied in conversion the SAR of a certain cell phone into field intensity and induced voltage to assess the effects of cell phone emissions on an implanted pacemaker. Cell phones will expose pacemakers to near-field radiation that is inversely proportional to (d^3).

4. Simulation results and discussion

Simulations were carried out using a MATLAB-based model to estimate the electromagnetic interference (EMI) induced in implanted cardiac pacemakers by 2G through 6G cell phones. The analysis considers power transmission, transmit antenna gain, burst factor, frequency band, and orientation angle between the cell phone antenna and the pacemaker lead. The effective lead length was assumed to be 20 cm, and the immunity threshold for the pacemaker was set to 3 V/m based on (AAMI)-PC69 standards [25] that are set by the Advancement of Medical Instrumentation.

Three orientation angles, 0°, 45°, and 90°, were studied at varying distances from 1 cm to 30 cm. Each simulation was performed under isotropic and directional radiation assumptions, corresponding to antenna characteristics of older mobile technologies generations (2G/3G) and newer generations (5G/6G), respectively.

Figure 3 illustrates the induced electric field at various distances and orientation angles (0°, 45°, 90°) for each cellular generation, where the power is assumed to be 2W transmitted through an isotropic antenna across all cell phone generations. At 0° alignment, 2G phones exhibit the highest EMI, with electric field intensity surpassing the threshold of 3 V/m within 15 cm. This is attributed to their lower frequency and continuous time-division multiple access (TDMA) burst emissions, which create persistent high-power peaks. Conversely, 5G and 6G phones demonstrate significantly reduced EMI, primarily due to: directional beamforming technique that can reduce the stray emissions; higher operational frequencies (mmWave/THz), which are subject to higher attenuation; and lower burst factors resulting in reduced exposure time. It can be noticed that at 45°orentation, the induced field is lower than that of zero degrees. At 90° orientation, the induced electric field decreases dramatically for all generations, confirming that the alignment between the phone antenna and pacemaker leads is a critically sensitive determinant of EMI risk.

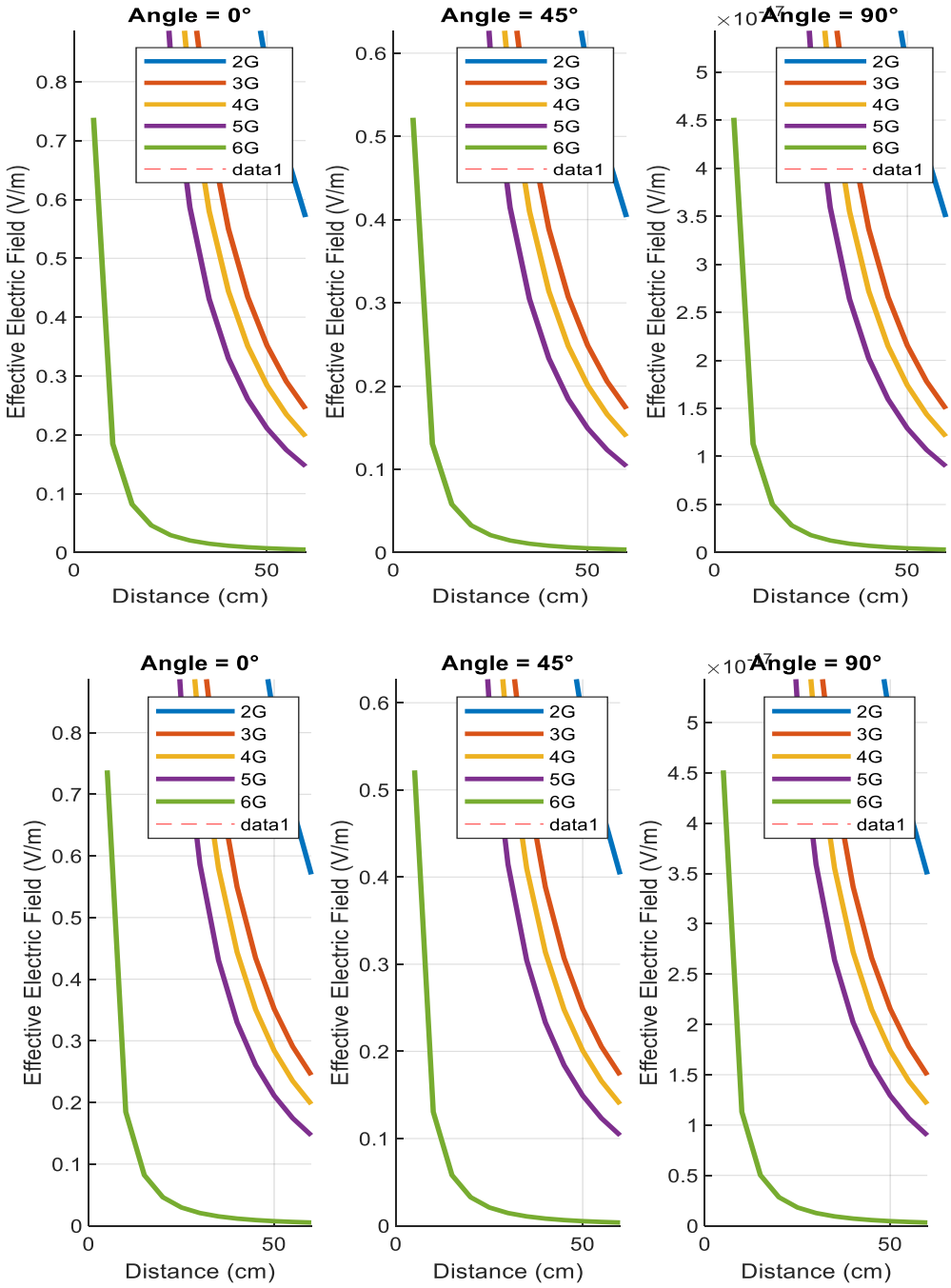

Figure 3. Field induced at different distances and angles

It can be noticed that a lower frequency of 2G cell phone produce relatively higher field strength at longer distances compared to 5G and 6G. This is because of lower path loss at lower frequencies. At closer distances (<20 cm) and 0° orientation, the electric field exceeds the threshold of 3 V/m, which has the potential to result in pacing inhibition in pacemakers. Furthermore, it can be noticed that the induced electric field drops with increasing orientation angle, and the greatest risk occurs where there is direct alignment. At mmWave (5G) and THz (6G) bands, signal attenuation is severe with distance; therefore, EMI due to 5G/6G cell phones is rapidly diminished, making 5G and 6G less dangerous unless the phone is extremely close and aligned directly with the device.

Figure 4 summarizes the EMI risk matrix across generations. It clearly highlights that high-risk zones for 2G/3G located within 10-15 cm at direct orientation. 2G/3G cell phones are more likely to produce high-risk zones at close distances, while 5G and 6G are usually safe, even at 5-10 cm, unless oriented directly (0°). For 4G, EMI

risk is moderate but may still exceed thresholds at very close proximity (≤5 cm). Additionally, safe zones for 5G/6G at almost all tested distances indicate strong electromagnetic compatibility unless alignment is direct and extremely close (<2 cm).

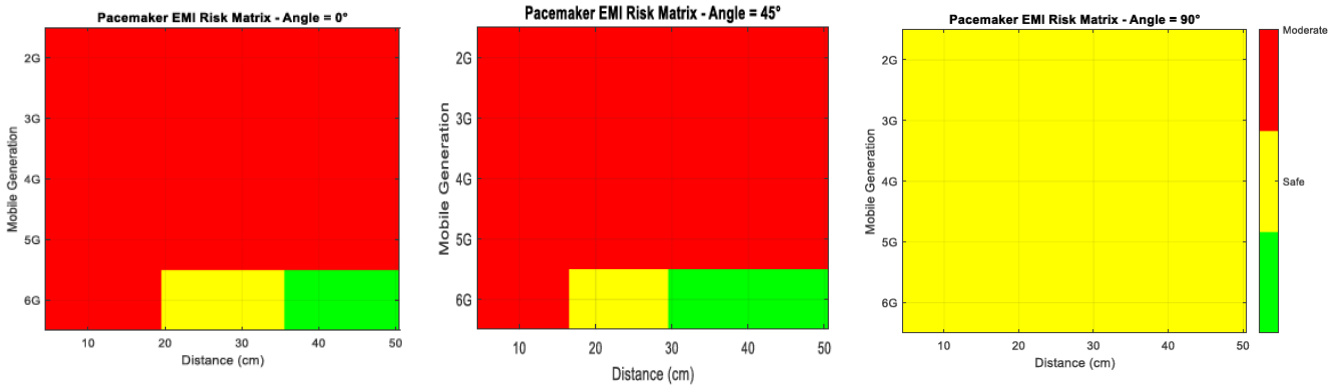

Figure 4. Risk matrix at different angles

Another simulation depends on the phone generation specifications explained in Table 1, was conducted to assess the interference intensity (EMI) and the induced voltage across different cell phone generations. The distance between the cell phone and the pacemaker varied from 1.0 cm to 30 cm, and the orientation angle is changed from 0 to 180 degrees for each generation. The findings reinforce that interference potential across cell phone generations is highly dependent on both spatial distance and orientation angle, as illustrated in Figure 5.

The simulation results show that there is an inverse relationship between the cell phone generation and the produced interference intensity. Older cell phone generations produce higher interference intensity, while newer generations pose little to no significant interference. The interference effect is highly sensitive to the physical separation distance between the cell phone and the pacemaker. The effect is reduced due to the inverse square law. This explains that maintaining a safe separation distance between the mobile phone and pacemaker is an effective protective method in interference effect reduction.

The interference risk is highest when the pacemaker is located in front of the cell phone antenna. This orientation factor is modeled by a cosine function and reflects the antenna directivity. It can be noticed that the interference effect drops significantly at angles beyond 60°, confirming that the phone orientation angle relative to the body is an important factor. Furthermore, it can be noticed that the older generation (2G and 3G) is characterized by higher induced field strengths and pulsed transmissions, leading to higher EMI, while the newer generation of lower burst factors and less EMI footprint. It is recommended to keep cell phones at least 15 cm away from implanted cardiac devices, especially for older generation phones. The results also remarked that newer cell phone technologies, 5G and 6G, demonstrate negligible risk even at short distances, which means that electromagnetic compatibility is improved in these generations.

Table 1. Description of cell phone generation specifications [3, 17]

Phone Generation	Electric Field at 10 cm (V/m)	Burst Factor B	Frequency Band	Modulation	Pulse Frequency
2G	15	1.5	900-1800 MHz	TDMA	217 Hz pulse
3G	10	1.2	2.1 GHz	CDMA/WCDMA	Spread spectrum
4G	8	1.0	700MHz-2.6GHz	OFDMA	Less pulsed
5G	5	0.6	3.5GHz-28GHz	OFDM	Directional
6G	2	0.3	100-300GHz	AI Optimized	Highly directional

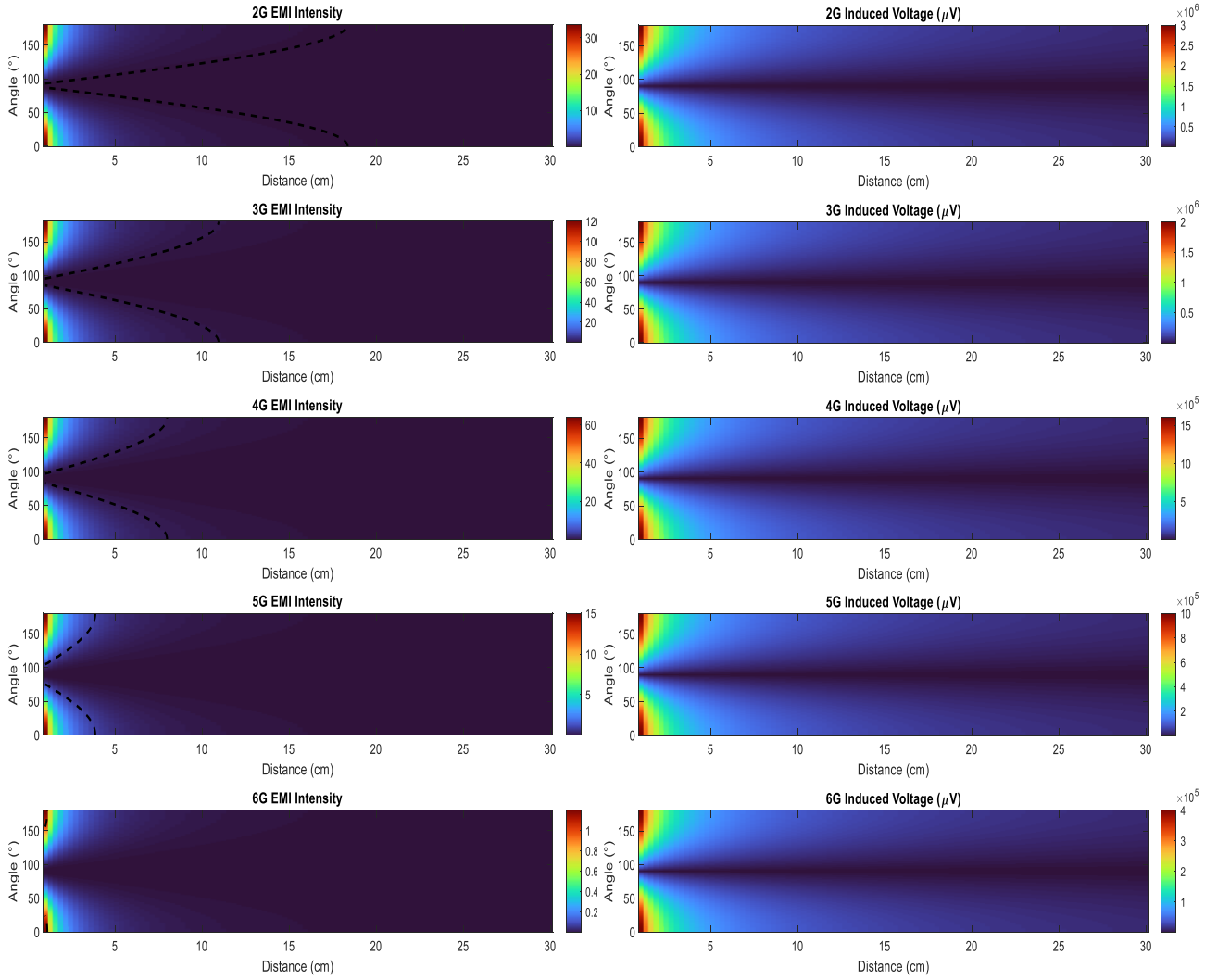

Figure 5. Effects of EMI on different generations

At the next simulation, a cell phone with SAR of 1.4 W/kg is chosen to be the EMI source while the cardiac muscle tissue with a conductivity of 1.5 S/m is assumed to be near the victim's pacemaker. The field intensity and the induced voltage at pacemaker leads are plotted against the near-field distance that varies from 0.5cm to 5.0 cm, as shown in Figure 6.

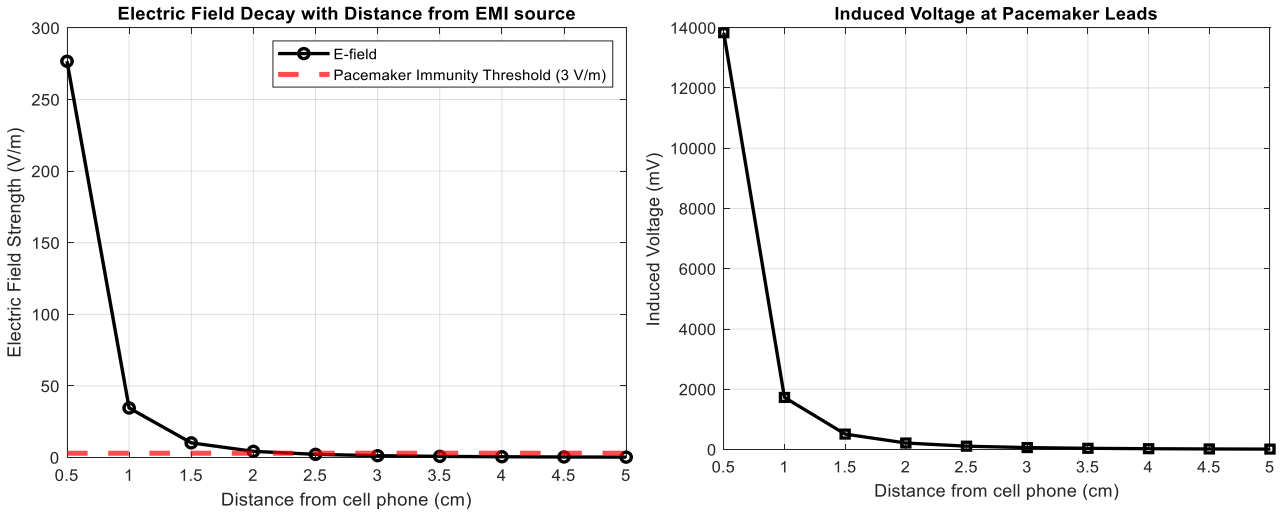

Figure 6. Effects of the near–field of a cell phone with known SAR

A secondary simulation used SAR values to estimate near-field electric fields. Using typical SAR ratings from commercially available devices, iPhone 15 Pro (0.99 W/kg), Samsung S23 Ultra (1.35 W/kg), and Galaxy S24 (1.14 W/kg), the corresponding electric fields were computed. Figure 6 demonstrates that induced fields remain within safety limits defined by AAMI (20 V/m) and the International Committee of Non-Ionizing Radiation Protection ICNIRP (61 V/m) beyond 2 cm for all phones. For most recent phones, induced electric fields remain <10 V/m at distances >1.5 cm. Figure 7 shows the electric field induced due to three cell phones of different rated SAR values. It can be concluded that modern cell phones pose minimal risk if kept at a distance ≥15 cm from pacemakers, or simply the ear opposite the implanted pacemaker can be used. The findings of this study can be exploited with filters [26, 27], antennas [28, 29], diplexers [30], and machine learning [31, 32].

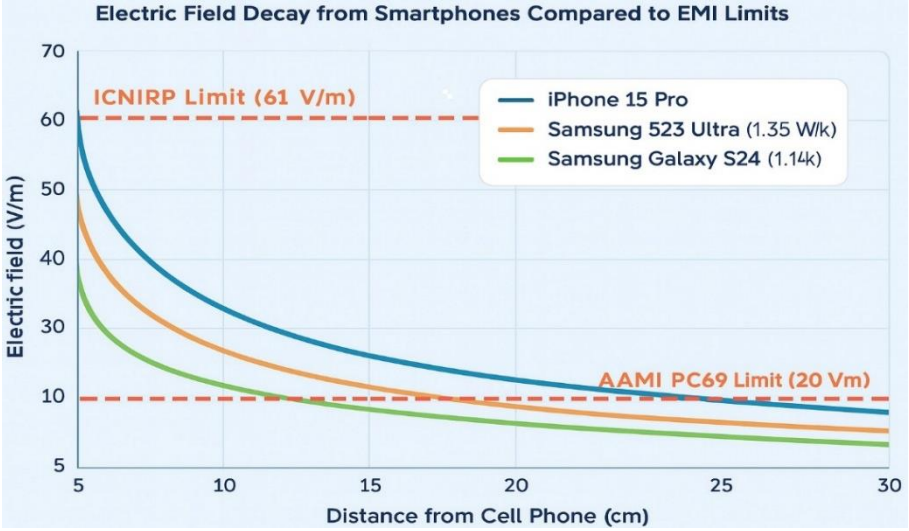

Figure 7. Effects of the near-field of three cell phones

5. Conclusions

This study developed a comprehensive modeling and simulation framework to assess electromagnetic interference from 2G to 6G mobile phones on implanted pacemakers. Results indicate that 2G and 3G phones may exceed the safety threshold of 3 V/m at close proximities (<15 cm), particularly under direct alignment. In contrast, 5G and 6G phones exhibit significantly lower EMI potential due to directional transmission and higher frequency-induced path loss. The proposed model provides insights into EMI behavior across orientations and frequencies, and it supports the update of safety standards and testing protocols. Future work may focus on incorporating real-body phantoms and validating simulation results through experimental setups.

Declaration of competing interest

The authors declare that they have no known financial or non-financial competing interests in any material discussed in this paper.

Funding information

The authors declare that they have received no funding from any financial organization to conduct this research.

Author contribution

Jaafar Qassim Kadhim: Conceptualization of the study, design of the microstrip bandpass filter, and writing of the original draft.

Hassan Hamed Naji: Conducted simulations and analysis of the filter performance, contributed to the methodology, and assisted in manuscript preparation.

Sazan K. AL-jaff: Supervised the project, provided critical revisions to the manuscript, and ensured the integrity of the research.

References

[1] S. J. Seidman, P. S. Ruggera, R. G. Brockman, B. Lewis, and M. J. Shein, "Electromagnetic compatibility of pacemakers and implantable cardiac defibrillators exposed to RFID readers," Int. J. Radio Freq. Identif. Technol. Appl., vol. 1, no. 3, pp. 237–246, 2007. https://doi.org/10.1504/IJRFITA.2007.015848.

[2] T. Hamed and M. Maqsood, "SAR calculation & temperature response of human body exposure to electromagnetic radiations at 28, 40, and 60 GHz mmWave frequencies," Prog. Electromagn. Res. M, vol. 73, pp. 47–59, 2018. https://doi.org/10.2528/PIERM18061102.

[3] T. Wisaratapong, N. Pechaksorn, T. Liabsuetrakul, and W. Lohawijarn, "The Effect of Electromagnetic Interference Produced by Smartphones Using 5G Network on Patients With Permanent Pacemakers (EMS5G-PPM Study)," J. Interv. Cardiol., vol. 2024, no. 1, p. 3550004, 2024. https://doi.org/10.1155/2024/3550004.

[4] IEEE Standards Coordinating Committee, "IEEE standard for safety levels with respect to human exposure to radio frequency electromagnetic fields, 3 kHz to 300 GHz," IEEE C95.1-1991, 1992.

[5] F. Al-Fadhli, Z. Al-Araji, N. Swaikat, A. Muratov, and A. Turetsky, "The perfect position of electrical components on PCBs in the communication system industry from the mechanical aspects' viewpoint," J. Mech. Eng. Res. Dev., vol. 43, no. 4, pp. 82–91, 2020.

[6] J. Werner and L. Nolle, "Spice model generation from EM simulation data using integer coded genetic algorithms," in Proc. Int. Conf. Innov. Tech. Appl. Artif. Intell., Springer, pp. 355–367, 2016. https://doi.org/10.1007/978-3-319-47175-4_26.

[7] Y. Li and M. Lu, "Study on SAR distribution of electromagnetic exposure of 5G mobile antenna in human brain," J. Appl. Sci. Eng., vol. 23, no. 2, pp. 279–287, 2020. https://doi.org/10.6180/jase.202006_23(2).0012.

[8] International Commission on Non-Ionizing Radiation Protection (ICNIRP), "Guidelines for limiting exposure to electromagnetic fields (100 kHz to 300 GHz)," Health Phys., vol. 118, no. 5, pp. 483–524, 2020. https://doi.org/10.1097/HP.0000000000001210.

[9] A. H. Sallomi, "A theoretical approach for SAR calculation in human head exposed to RF signals," J. Eng. Sustain. Dev., vol. 16, no. 4, pp. 304–313, 2012.

[10] H. T. S. ALRikabi, A. H. Sallomi, H. F. KHazaal, A. Magdy, I. Svyd, and I. Obod, "A Dumbbell Shape Reconfigurable Intelligent Surface for mm-wave 5G Application," Int. J. Intell. Eng. Syst., vol. 17, no. 6, 2024.

[11] A. H. Sallomi, S. A. Hashim, and M. H. Wali, "SAR and thermal effect prediction in human head exposed to cell phone radiations," Cell, vol. 1, pp. 12–15, 2018.

[12] M. D. H. Almawlawe, M. Al-badri, and I. H. Alsakini, "Performance improvement of a DC/DC converter using neural network controller in comparison with different controllers," IOP Conf. Ser.: Mater. Sci. Eng., vol. 870, no. 1, p. 012119, 2020. https://doi.org/10.1088/1757-899X/870/1/012119.

[13] E. Hanada, Y. Watanabe, and Y. Nose, "Electromagnetic interference with electronic medical equipment induced by automatic conveyance systems," J. Med. Syst., vol. 24, no. 1, pp. 11–20, 2000. https://doi.org/10.1023/a:1005424910489.

[14] O. Gutiérrez, M. Á. Navarro, F. S. de Adana, A. Escobar, M. E. Moncada, and C. M. Muñoz, "Study of electromagnetic compatibility in hospital environments," J. Electromagn. Anal. Appl., vol. 6, no. 07, p. 141, 2014. https://doi.org/10.4236/jemaa.2014.67015.

[15] I. Baba et al., "Experimental study of electromagnetic interference from cellular phones with electronic medical equipment," J. Clin. Eng., vol. 23, no. 2, pp. 122–134, 1998.

[16] W. M. Hashim and A. H. Sallomi, "Broadband Microstrip Antenna for 2G/3G/4G Mobile Base Station Applications," Al-Qadisiyah J. Eng. Sci., vol. 11, no. 2, pp. 165–175, 2018.

[17] T. S. Rappaport, Wireless Communications: Principles and Practice, 2nd ed. Pearson Education India, 2010.

[18] P. M. Mariappan, D. R. Raghavan, S. H. A. Aleem, and A. F. Zobaa, "Effects of electromagnetic interference on the functional usage of medical equipment by 2G/3G/4G cellular phones: A review," J. Adv. Res., vol. 7, no. 5, pp. 727–738, 2016. https://doi.org/10.1016/j.jare.2016.07.001.

[19] A. Klein and G. Djaiani, "Mobile phones in the hospital–past, present and future," Anaesthesia, vol. 58, no. 4, pp. 353–357, 2003. https://doi.org/10.1046/j.1365-2044.2003.03196.x.

[20] J. S. Seybold, Introduction to RF Propagation. John Wiley & Sons, 2005.

[21] C. A. Balanis, Antenna Theory: Analysis and Design, 4th ed. John Wiley & Sons, 2016.

[22] K. Fujimoto, Mobile Antenna Systems Handbook. Artech House, 2001.

[23] S. Kim and I. Nasim, "Human electromagnetic field exposure in 5G at 28 GHz," IEEE Consum. Electron. Mag., vol. 9, no. 6, pp. 41–48, 2020. https://doi.org/10.1109/MCE.2019.2956223.

[24] J. Lin, J. Li, and G. Ding, "Absorption of 5G sub-6 GHz electromagnetic radiation from base station to male reproduction system," Int. J. Radiat. Biol., vol. 100, no. 7, pp. 1085–1092, 2024. https://doi.org/10.1080/09553002.2024.2347354.

[25] B. Alpert, B. Friedman, and D. Osborn, "AAMI blood pressure device standard targets home use issues," Biomed Instrum Technol., vol. 69, 2010.

[26] Y. S. Mezaal, H. T. Eyyuboglu, and J. K. Ali, "Wide bandpass and narrow bandstop microstrip filters based on Hilbert fractal geometry: Design and simulation results," PLOS ONE, vol. 9, no. 12, pp. 1–18, Dec. 2014. https://doi.org/10.1371/journal.pone.0115412.

[27] Y. S. Mezaal, H. T. Eyyuboglu, and J. K. Ali, "New dual band dual-mode microstrip patch bandpass filter designs based on Sierpinski fractal geometry," in Proc. 3rd Int. Conf. Adv. Comput. Commun. Technol. (ACCT), IEEE, pp. 348–352, 2013. https://doi.org/10.1109/ACCT.2013.72.

[28] N. Ali, A. Mohammed, H. ALRikabi, A. Aliwy, and H. Khazaal, "Development and implementation of a microstrip antenna for autonomous vehicles and IoT in 5G communication systems," J. Appl. Res. Technol., vol. 22, no. 6, pp. 816–822, 2024. https://doi.org/10.22201/icat.24486736e.2024.22.6.2627.

[29] B. K. Al-Shammari et al., "Design of a High Gain Yagi-Uda Antenna Array for VHF-Band Radar Applications," Eng. Technol. Appl. Sci. Res., vol. 14, no. 5, pp. 17188–17195, 2024.

[30] K. Al-Majdi and Y. S. Mezaal, "New miniature narrow band microstrip diplexer for recent wireless communications," Electronics, vol. 12, no. 3, p. 716, 2023. https://doi.org/10.3390/electronics12030716.

[31] M. S. Shareef, T. Abd, and Y. S. Mezaal, "Gender voice classification with huge accuracy rate," Int. J. Intell. Eng. Syst., vol. 18, no. 5, pp. 2612–2617, 2020.

[32] R. J. Kadhim, F. S. Al-Juboori, and H. J. N. Alsaedi, “Driven gamification by AI in a time series healthcare case study: Statistical intervention analysis,” Sustain. Eng. Innov., vol. 7, no. 2, pp. 345–354, 2025. https://doi.org/10.37868/sei.v7i2.id560.